

USING A MODIFIED LANE'S RELATION IN LOCAL BED SCOURING STUDIES IN ALUVIAL BED

Marta Kiraga, Zbigniew Popek

Warsaw University of Life Sciences – SGGW

Abstract. Numerous approaches to the local scour studies have been developed. The research aim was to verify modified Lane's relation in scope of local scouring phenomenon basing on laboratory studies results. Original Lane's relation [1955] is applicable in dynamic balance conditions in alluvial rivers context. Original form is not an equation, but a qualitative expression which cannot be directly used to estimate the influence of a change in one parameter on the magnitude of others. Modified version allows transforming it into equation for dynamic equilibrium conditions in steady flow assumption and gives a new opportunity to this principle application. Two physical models of laboratory channel with rectangular cross-sections and glass panels have been constructed, with totally or partially sandy bottom. Model I assumed non-continual sediment transport, because of model construction, i.e. the solid bottom transforms into sandy bottom in the intake part. Model II assumed water structure (the weir with four slots) introducing into laboratory channel with solid bottom in its region, whereas the rest of channel was filled with sand above and below structure, i.e. continuity of sediment transport was assured. Results of research confirmed modified Lane's relation usability in scope of local scouring phenomenon description in dynamic equilibrium conditions of alluvial sandy bed.

Keywords: local scour, dynamic balance, Lane's relation, physical modelling, alluvial rivers

INTRODUCTION

Numerous approaches to the local scour forming studies have been developed [Aderibigbe and Rajaratnam 1998, Dąbkowski and Siwicki 2000, Lenzi et al. 2002, Gaudio and Marion 2003, Siwicki & Urbański 2004, Melville 2008, Siwicki 2008, Kiraga and Popek 2016] both on the grounds on laboratory research and *in-situ* data. The

Corresponding Authors: mgr inż. Marta Kiraga, dr hab. inż. Zbigniew Popek, prof. SGGW, Warsaw University of Life Sciences – SGGW, Water Engineering Division, Department of Hydraulic Engineering, 159 Nowoursynowska Street, Post code 02-787, Warsaw, Poland; e-mail: marta_kiraga@sggw.pl.

© Copyright by Wydawnictwo Uniwersytetu Rolniczego w Krakowie, Kraków 2016

present research reveals different scientific approach to the local scouring phenomenon. Lane's relation [1955] is applied in laboratory studies, used commonly in alluvial rivers morphology forming context. River channel and valley forming process is the outcome of water flow and sediment transport mutual influence, tending to obtain an dynamic equilibrium (stability) of the channel [Popek 2006]. Natural river stays in equilibrium conditions if in a long period of time basic flow parameters, such as even longitudinal river decline, average channel width and depth, and bedload granulation's characteristics remain constant, what is originally described by Lane. Lane's relation of fluvial hydraulics is derived from basic principles of sediment transport:

$$Q_s \cdot d \sim Q_w \cdot S \quad (1)$$

where:

- Q_s – sediment transport discharge, $\text{m}^3 \cdot \text{s}^{-1}$,
- d – particle diameter, m,
- Q_w – water discharge, $\text{m}^3 \cdot \text{s}^{-1}$,
- S – energy grade line slope.

Lane's relation is not an equation, but a qualitative expression which cannot be directly used to estimate the influence of a change in one parameter on the magnitude of others, however despite its qualitative and simplified character, serves well to describe the nature of the process of forming alluvial stream channels. Proportion sign points that change in any of the four variables will cause a change in the others such that equilibrium is restored. Results of many field studies, as well as analyses of causes and effects of the river's loss of dynamic balance, support the assumptions of Lane's relation with which one can predict tendencies in changes of hydraulic and morphological characteristics of stream channels [Hickin 1977, Schumm 1977, Brookes 1988, Church 1992, Warburton et al. 2002].

It was attempted to describe more precise the river morphology forming process, using classic Lane's relation, according to Lane's sentence [1955]: "The science of fluvial morphology has developed from two roots which have been largely independent of each other". Geology and engineering – these two roots have remained largely separate down to the present time. Scientists [Dust and Wohl 2012] focused on one of these roots: geology, but the second – engineering – is up to now insufficiently studied and needs wider description. Concomitantly, the Lane's relation in scope of local scouring in laboratory conditions has not been examined yet. The present paper consist on one of the other scientist's Lane's relation modification [Schumm 1969, Huang et al. 2014] (Eq. 2), considering width-to-depth ratio in modified relation.

$$Q_w \cdot S \sim Q_s \cdot d \cdot \left(\frac{W}{H}\right)^{-1} \quad (2)$$

where:

- $\left(\frac{W}{H}\right)$ – width-to-depth ratio.

To describe equilibrium conditions in scope of scouring phenomenon, local scours are classified into two categories – clear-water scour and live-bed scours. Clear water scour occurs when the bed material is not in motion and the sediment load transported into the contracted section is essentially zero. Clear-water scour occurs when the shear stress induced by the water flow exceeds the critical shear stress of the bed material. Live-bed scour occurs when the scour hole is continuously fed with sediment by approaching flow [Barbhuiya and Dey 2004]. By itself, a live bed will not cause a scour hole – for this to be created some additional increase in shear stress is needed, such as that caused by a contraction or a local obstruction. Equilibrium conditions during local scour deepening can be recognized through maximal scour depth comparison in subsequent time steps [Chabert and Engeldinger 1956] (Fig. 1).

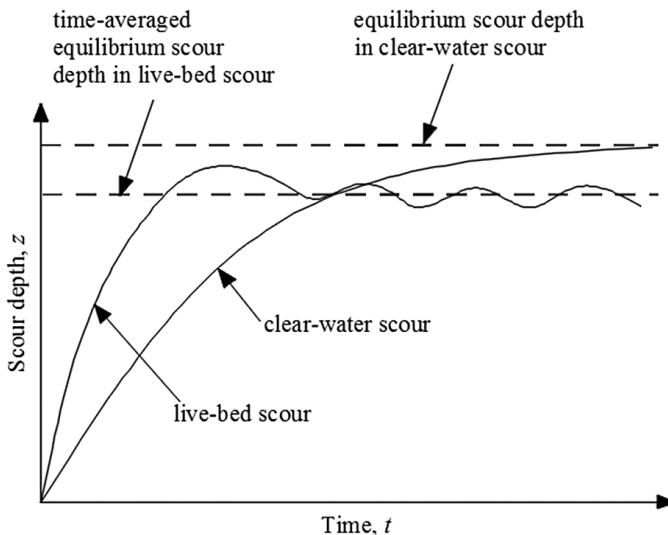


Fig. 1. Time development of clear-water and live-bed scour [Chabert and Engeldinger 1956]

The paper presents further modification of Lane's relation, verified both in clear-water and live-bed scour equilibrium conditions on two models of laboratory channel structure with steady flow assumption.

METHODOLOGY

The Modified Lane's Relation

Because the lack of consistency of parameters on the left and the right side of original Lane's relation (Eq. 1), there is no opportunity to use it to the functional description of bedload's dynamic balance conditions. In order to eliminate this inconvenience, the relation modification is suggested, which relies on the replacement of sediment d design grain size with dimensionless grain parameter D_* [Kiraga and Popek 2016], described by Bonnefille with the following relation [Van Rijn 1993]:

$$D_* = d_{50} \cdot \left[\frac{(s-1)g}{\nu^2} \right]^{1/3} \quad (3)$$

where:

- d_{50} – mass median grain diameter, m,
- s – specific density of solid particles; $s = \rho_s \cdot \rho_w^{-1}$, where: ρ_s – bed material specific density, $\text{kg} \cdot \text{m}^{-3}$, ρ_w – water specific density, $\text{kg} \cdot \text{m}^{-3}$,
- g – acceleration of gravity, $\text{m} \cdot \text{s}^{-2}$,
- ν – kinematic viscosity parameter, $\text{m}^2 \cdot \text{s}^{-1}$.

D_* parameter introduction into relation leads to an units accordance obtainment, therefore a proportion sign could be replaced with equality sign. Modified Lane's relation derived from original form and Huang et al. [2014] adjustment eventually takes the following form with D_* parameter included [Kiraga and Popek 2016]:

$$Q_s \cdot D_* \cdot \left(\frac{W}{H} \right)^{-1} = Q_w \cdot S \quad (4)$$

Description of test stand

The aim of the research was to examine the possibility to use the modified Lane's relation for two models of laboratory channel structure, with solid and sandy bed part, filled with sand with mass median diameter of grain $d_{50} = 0.62$ mm, where the local scour was forming. Every single experiment was performed during t_i total time, just to obtain the stable shape and achieve an dynamic equilibrium both in clear-water and live-bed conditions. Studies were conducted in 8.0 meters length, about 1.0 meter height and 0.58 meters width W laboratory channel with rectangular cross-section. A pin water gauge was used in the intake part in order to measure the water surface elevation in asumed time steps, regulated with a gate. In order to measure the ordinate of water surface level in these time steps a moving pin water gauge was used which was placed on the trolley pushed on guides along the channel. The level of the sandy bottom within the washout bed was measured with a moving disc probe in presumed cross-sections. The water flow discharge was examined with the use of electromagnetic flow meter. The specific density of sand ρ_s in the washout bed was $2610 \text{ kg} \cdot \text{m}^{-3}$. Therefore, assuming a water density ρ_w on the level of $1000 \text{ kg} \cdot \text{m}^{-3}$, the specific density of solid particles was estimated at $s = 2.61$ [Kiraga and Popek 2016]. No additional sediment feeding system was adopted in both models.

First model (I) consist on following bottom construction: about 4-meter length solid bottom transforms into 2.18 meters length sandy bottom in the intake part (Fig. 2). Due to the increase of flow resistance on the whole length of the bed, resulting from varied roughness of solid and sandy bottom, the hydraulic gradient increases causing the increase of shear stress on the bottom. After exceeding the critical shear stress, the motion of sediment grains begins and is followed by gradual scour of the bed during the time of experiment until the shape and the parameters of local scours stabilize. Then, the local

scour obtains its equilibrium depth in clear-water scour conditions z_{max} because no sediment feeding system application (Fig. 3). The experimental conditions in this study may be compared to a case of the transport continuity being disrupted by the accumulation of the bedload material in retention reservoir located in the upstream [Dust and Wohl 2012, Huang et al. 2014].

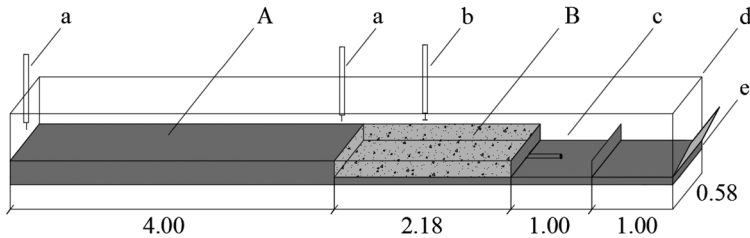


Fig. 2. Experimental channel scheme – model I (all dimensions in meters), where: A – solid bottom, B – washout bed (sandy); a – pin water gauge, b – disc probe, c – collection chamber, d – glass panels, e – the regulatory gate [Kiraga and Popek 2016]

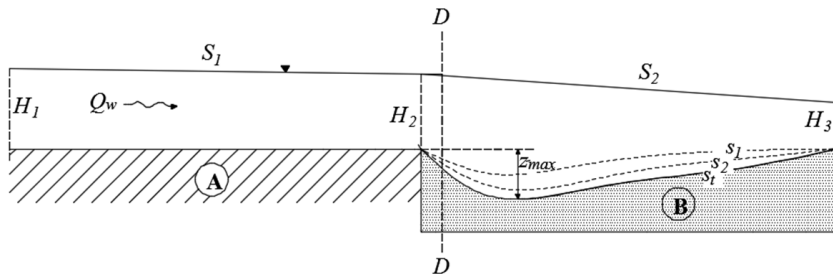


Fig. 3. Scheme of local scour forming in washable area of sandy bed in model I, where: A – solid bottom; B – sandy washout bed; $D-D$ – computational cross-section, H_1 , H_2 , H_3 – water depth; Q_w – water flow discharge; S_1 , S_2 – energy grade line slope; z_{max} – maximal depth of local scour while achieving stabilization in time t_t with s_t scour shape (clear-water equilibrium scour depth); s_1 , s_2 , s_t – shapes of bed while duration of experiment in time [Kiraga and Popek 2016]

The second model (II) assumed water structure introduction – the weir made of stone with four slots (summary area of slots $As = 0.035 \text{ m}^2$). A solid bottom was situated in the nearest region of the weir, whereas sandy washout bottom was situated below and above structure (Fig. 4, 5). Sandy bed above the structure was washed out by approaching flow and sediment load was moved out from upper part towards lower part of water structure, ensuring live-bed conditions. Damming up the channel causes significant energy grade line slope increment below the structure and also reinforcing the velocity of the water in structure's slots because of flow area reduction, therefore the shear stress increment on the bottom is the result not only of roughness variability in this case (Fig. 6). Local scour was gradually formed until live-bed equilibrium conditions were obtained, just to achieve stable shape and maximal depth z_{max} .

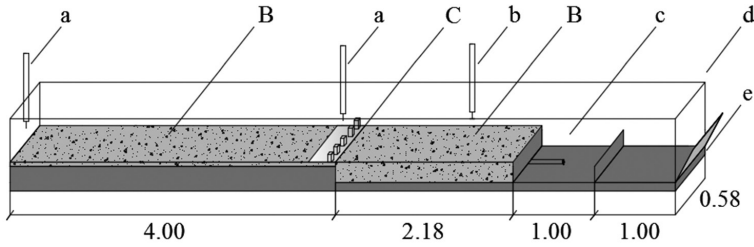


Fig. 4. Experimental channel scheme – model II (all dimensions in meters), where: B – washout bed (sandy), C – stone weir and solid bottom; a – pin water gauge, b – disc probe, c – collection chamber, d – glass panels, e – the regulatory gate

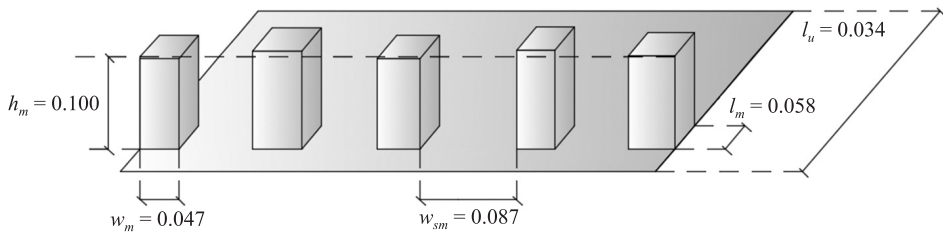


Fig. 5. Stone weir scheme, where h_m – medium water structures' single element height, m, w_m – medium weir's element width, m, w_{sm} – medium slot width, m, l_m – medium weir's element length, l_u – total length of solid bed nearby the weir, m

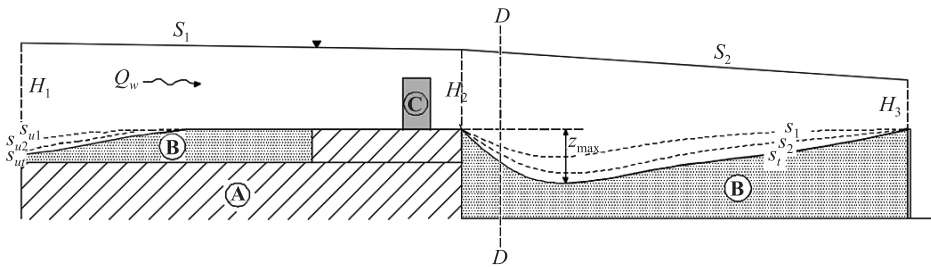


Fig. 6. Scheme of local scour forming in washable area of sandy bed in model II, where: A – solid bottom; B – sandy washout bed; C – stone weir; $D-D$ – computational cross-section, H_1, H_2, H_3 – water depth; Q_w – water flow discharge; S_1, S_2 – energy grade line slope; z_{max} – maximal depth of local scour while achieving stabilization in time t_1 with s_1 scour shape (live-bed equilibrium scour depth) and s_{u1} shape of the bottom above the weir; s_1, s_2, s_3 – shapes of bed below the weir while duration of experiment in time; s_{u1}, s_{u2}, s_{u3} – shape of the bottom above the weir while duration of experiment in time

Scope of the study

Modified Lane's relation parameters were accomplished during each experiment. Steady water flow discharge and water surface elevation were verified in 13 variants of discharge ($Q_w = 0,020 - 0,045 \text{ m}^3 \cdot \text{s}^{-1}$) and depth ($H = 0,10 - 0,20 \text{ m}$) for each model. When equilibrium conditions were reached in total time t_p , i.e. no visible particle movement in subsequent time steps, the flume was drained carefully and the volume of sand captured in the collection chamber V_t was measured, providing information on the total volume of scour, that could be easily transformed into sediment transport discharge Q_s dividing by total time t_t . Besides washout bed shape and water surface elevation, temperature was measured in each time step during each experiment, that allows kinematic viscosity parameter obtainment and Bonnefille's parameter D_* calculation (Eq. 3) (Tab. 1, 2) [Kiraga and Popek 2016].

Table 1. The summary table of measurement's parameters for model I of model structure [Kiraga and Popek 2016]

Number of measurement	Q_w $\text{m}^3 \cdot \text{s}^{-1}$	H m	T $^{\circ}\text{C}$	ν $1 \cdot 10^{-6} \cdot \text{m}^2 \cdot \text{s}^{-1}$	D_* –	V_s m^3	t_t h	z_{\max} cm
1	0.020	0.10	16.8	1.086	14.72	0.00153	7.25	0.36
2	0.025	0.10	16.5	1.094	14.65	0.01841	10.50	2.00
3	0.025	0.12	16.1	1.104	14.56	0.00151	6.50	0.41
4	0.030	0.10	16.5	1.094	14.65	0.03701	5.00	3.75
5	0.030	0.15	16.7	1.089	14.70	0.00151	6.00	0.30
6	0.035	0.12	16.3	1.099	14.61	0.04681	8.50	4.25
7	0.035	0.15	15.9	1.109	14.52	0.00404	7.50	1.22
8	0.040	0.10	16.0	1.107	14.54	0.09746	9.25	10.61
9	0.040	0.12	17.2	1.076	14.81	0.05500	10.50	7.89
10	0.040	0.15	17.0	1.081	14.77	0.01900	8.00	2.37
11	0.040	0.20	16.8	1.086	14.72	0.00240	6.00	0.39
12	0.043	0.12	16.6	1.091	14.68	0.06800	8.50	6.18
13	0.045	0.15	16.0	1.107	14.54	0.04500	8.50	4.41

To recognize better the hydraulic conditions, Froude number was also calculated for initial conditions in time $t = t_0$ right before local scour formation on the grounds on calculated water flow velocity u . Froude number was calculated for computational D - D cross section for model I and in weir region for model II, considering u velocity in structure's slots.

$$Fr = \frac{u}{\sqrt{g \cdot H}} \quad (5)$$

Table 2. The summary table of measurement's parameters for model II of model structure

Number of measurement	Q_w	H	T	ν	D_*	V_s	t_t	z_{\max}
	$\text{m}^3 \cdot \text{s}^{-1}$	m	$^{\circ}\text{C}$	$1 \cdot 10^{-6} \cdot \text{m}^2 \cdot \text{s}^{-1}$	–	m^3	h	cm
1	0.020	0.10	16.0	1.107	14.54	0.01000	8.00	6.13
2	0.025	0.10	16.8	1.086	14.72	0.04800	8.00	8.72
3	0.025	0.12	16.0	1.107	14.54	0.01400	8.00	5.92
4	0.030	0.10	16.7	1.089	14.70	0.07480	8.00	8.43
5	0.030	0.15	16.8	1.086	14.72	0.00040	8.00	2.70
6	0.035	0.12	16.8	1.086	14.72	0.07900	8.00	8.09
7	0.035	0.15	16.6	1.091	14.68	0.01340	8.00	4.72
8	0.040	0.10	16.3	1.099	14.61	0.11200	8.00	8.70
9	0.040	0.12	17.0	1.081	14.77	0.10200	8.00	8.26
10	0.040	0.15	16.3	1.099	14.61	0.03600	8.00	5.16
11	0.040	0.20	16.8	1.086	14.72	0.00065	8.00	1.42
12	0.043	0.12	16.7	1.089	14.70	0.14452	8.00	8.68
13	0.045	0.15	16.1	1.104	14.56	0.06000	8.00	2.35

Q_w – water flow discharge, H – depth in the channel in control profile, T – average temperature of water, ν – kinematic viscosity parameter, D_* – Bonnefille's dimensionless grain parameter, V_s – total scour volume, t_t – duration of measurement, z_{\max} – maximal (equilibrium) scour depth

It was also analysed the comparison between dimensionless shear stress in bed region θ and critical shear stress (Shield number) θ_{cr} . Because in any case of experimental variant there was a scour formed *i.e.* it was visible movement of particles during research until stable scour shape obtainment, it was expected to fulfil the requirement $\theta > \theta_{cr}$.

$$\theta = \frac{\tau_b}{(\rho_s - \rho_w) g \cdot d_{50}} \quad (6)$$

where:

τ_b – bed shear stress (Pa), calculated for hydraulic radius R_b of the sandy bottom part in cross section and energy grade line slope S_0 measured in the lower part of the weir, in time $t = t_0$, as it follows:

$$\tau_b = \rho_w \cdot g \cdot R_b \cdot S_0 \quad (7)$$

To determine the R_b value in chosen cross section Einstein division of velocity field was used [Horton 1933, Indlekofer 1981]. The hydraulic resistance and roughness coefficients change alongside the wetted perimeter of the chosen cross section in flume, what influences on shear stress distribution in cross section [Kubrak and Nachlik 2003]. Einstein method predicates the assumption of velocity distribution in cross section with

A_i areas, that is dependent on mutual relation between total value of hydraulic resistance for cross section and hydraulic resistances for separated part of wetted perimeter of cross section (Fig. 7):

$$\lambda = \frac{\sum \lambda_i \cdot O_i}{\sum O_i} \quad (7)$$

where:

- λ – total hydraulic resistance coefficient for cross section,
- λ_i – hydraulic resistance coefficient for the separate part of cross section with an absolute roughness k_{si} , m;
- O_i – wetted perimeter of separate part of cross section, m.

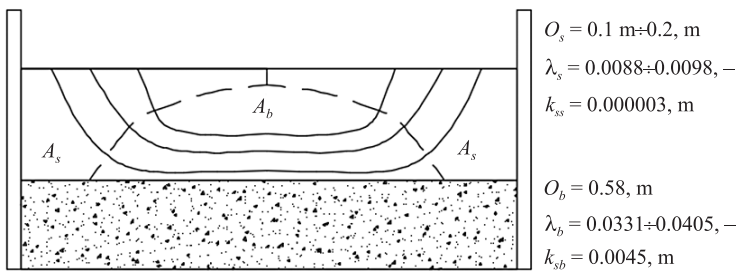


Fig. 7. Einstein's velocity field division scheme, where A_s – velocity field connected with glass panels with O_s wetted perimeter and λ_s hydraulic resistance coefficient for the separate part of cross section made of glass with an absolute roughness k_{ss} ; A_b – velocity field connected with sandy bed with O_b wetted perimeter and λ_b hydraulic resistance coefficient for the sandy bed with an absolute roughness k_{sb}

In accordance with Einstein's hypothesis, it is assumed that the mean velocity in total velocity field u is equal to velocity in separate part of total velocity field, i.e. in zones of water flow influence on bottom u_b and walls of the channel u_s . Analysis was performed for data obtained in the lower part of the weir, right before local scour formation in time $t = t_0$. With assumption of roughness equality of both walls in the cross section, there are fulfilled following relations:

- For mean velocity in each part of the cross section:

$$u = u_b = u_s \quad (8)$$

and

$$\frac{1}{\sqrt{\lambda}} \sqrt{8 \cdot g \cdot R \cdot S_0} = \frac{1}{\sqrt{\lambda_b}} \sqrt{8 \cdot g \cdot R_b \cdot S_0} = \frac{1}{\sqrt{\lambda_s}} \sqrt{8 \cdot g \cdot R_s \cdot S_0} \quad (9)$$

where:

- $\lambda, \lambda_b, \lambda_s$ – total hydraulic resistance coefficient for all velocity field, for the sandy bottom part of cross section and for glass walls

R, R_b, R_s – total hydraulic radius for all velocity field; hydraulic radius, that express impact of velocity field on the sandy bottom part; hydraulic radius, that express impact of velocity field on the single glass wall part, m.

- For cross section area: $A = 2A_s + A_b$, where: A – area of total velocity field, A_s – area of single velocity field, that impact on glass wall, A_b – area of velocity field, that impact on sandy bottom
- For hydraulic radius: $R = \frac{A}{O}, R_b = \frac{A_b}{O_b}, R_s = \frac{A_s}{O_s}$ where O, O_b, O_s – total wetted perimeter, wetted perimeter of the bottom part, wetted perimeter of the walls.

Hydraulic radiuses and hydraulic resistance coefficients for separate part of cross section were obtained from iterative calculations, using Colebrook-White equation:

$$\frac{1}{\sqrt{\lambda}} = -2 \log \left(\frac{2.51}{\text{Re} \sqrt{\lambda}} + \frac{k_s}{d \cdot 3.71} \right) \quad (10)$$

where:

k_s – absolute roughness, assumed as: $k_{sb} = 3d_{90} = 0.0045$ m [Van Rijn 1993] for the bottom and $k_{ss} = 3.0 \cdot 10^{-6}$ m for the glass walls [Bollrich and Preißler 1992] and Re is a Reynold's number (Fig. 7).

Shear stress in bed region θ was compared with Shield's number θ_{cr} , calculated for bed region as a function of local Reynold's number Re_* [Zanke 1982], dependent on median grain diameter d_{50} and water velocity in velocity field connected with bottom

region $u_* = \sqrt{\frac{\tau_b}{\rho_w}}$:

$$\text{Re}_* = \frac{d_{50} \cdot u_*}{\nu} \quad (11)$$

Then in accordance with Zanke [1982]:

$$\theta_{cr} = 0.432 \cdot \text{Re}_*^{-2} + 0.04(1 - 3.32 \cdot \text{Re}_*^{-1}) \quad (12)$$

Research includes attempt to correlate dimensionless shear stress in bed region θ in time $t = t_0$ with mean sediment discharge Q_s and with maximal scour depth z_{\max} for each measurement in time $t = t_r$.

RESULTS AND DISCUSSION

Maximal scour depth z_{\max} proceeding in subsequent time steps was analysed. Accordance of laboratory data with model curve was the basis for dynamic equilibrium conditions assurance for each laboratory research variant (Fig 1,8). While obtaining an equilibrium there was observed z_{\max} equality in subsequent time steps in clear-water conditions, meanwhile in live-bed there was a surplus of z_{\max} value in $t < t_r$, because of sediment load approaching from the upper part of model.

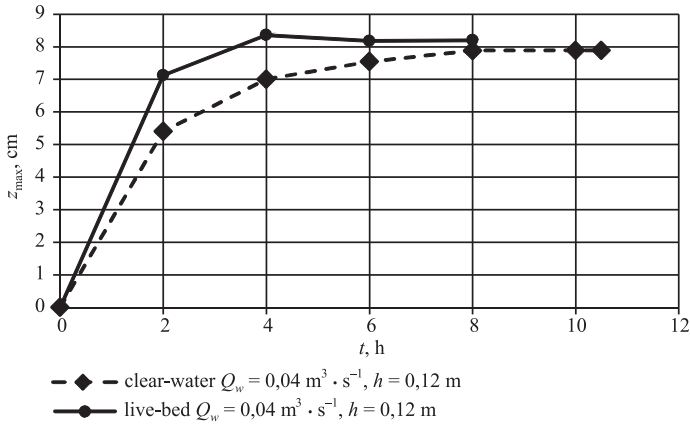


Fig. 8. Maximal scour depth z_{max} time development in clear-water (model I) and live-bed (II) conditions

Modified Lane's relation (Eq. 4) parameters were calculated for each variant of discharge and surface elevation in two models (Tab. 3, 4) with energy grade slope line assumption: $S = S_0$ for time $t = t_0 \cdot r^2$ correlation coefficient was calculated and line of the best fit was sketched for (x,y) points (Fig 9). Also linear functions' equations were stated (Eq. 14, 15).

$$\underbrace{Q_s \cdot D_* \cdot \left(\frac{W}{H}\right)^{-1}}_y = a \cdot \underbrace{Q_w \cdot S_0}_x \tag{13}$$

Table 3. Modified Lane's relations parameters for I model in clear-water equilibrium

Number of measurement	Q_w $m^3 \cdot s^{-1}$	H m	Q_s $(m^3 \cdot s^{-1}) \cdot 10^{-6}$	D_* -	$\left(\frac{W}{H}\right)^{-1}$ -	S_0 -	x $1 \cdot 10^{-6} \cdot m^3 \cdot s^{-1}$	y $1 \cdot 10^{-6} \cdot m^3 \cdot s^{-1}$
1	0.020	0.10	0.059	14.72	0.17	0.0005	10.00	0.15
2	0.025	0.10	0.487	14.65	0.17	0.0008	20.00	1.23
3	0.025	0.12	0.065	14.56	0.21	0.0004	10.00	0.19
4	0.030	0.10	2.056	14.65	0.17	0.0013	39.00	5.19
5	0.030	0.15	0.070	14.70	0.26	0.0004	12.00	0.27
6	0.035	0.12	1.530	14.61	0.21	0.0011	38.50	4.62
7	0.035	0.15	0.150	14.52	0.26	0.0005	17.50	0.56
8	0.040	0.10	2.927	14.54	0.17	0.0012	48.00	7.34
9	0.040	0.12	1.455	14.81	0.21	0.0010	40.00	4.46
10	0.040	0.15	0.660	14.77	0.26	0.0008	32.00	2.52
11	0.040	0.20	0.111	14.72	0.34	0.0002	8.00	0.56
12	0.043	0.12	2.222	14.68	0.21	0.0013	55.90	6.75
13	0.045	0.15	1.471	14.54	0.26	0.0008	36.00	5.53

Table 4. Modified Lane’s relations parameters for II model in live-bed equilibrium

Number of measurement	Q_w	H	Q_s	D_*	$\left(\frac{W}{H}\right)^{-1}$	S_0	x	y
	$m^3 \cdot s^{-1}$	m	$(m^3 \cdot s^{-1}) \cdot 10^{-6}$	–	–	–	$1 \cdot 10^{-6} \cdot m^3 \cdot s^{-1}$	$1 \cdot 10^{-6} \cdot m^3 \cdot s^{-1}$
1	0.020	0.10	0.347	14.54	0.17	0.0052	103.4	0.87
2	0.025	0.10	1.667	14.72	0.17	0.0066	165.3	4.23
3	0.025	0.12	0.486	14.54	0.21	0.0039	96.8	1.46
4	0.030	0.10	2.597	14.70	0.17	0.0059	177.0	6.58
5	0.030	0.15	0.014	14.72	0.26	0.0013	39.0	0.05
6	0.035	0.12	2.743	14.72	0.21	0.0061	213.5	8.35
7	0.035	0.15	0.465	14.68	0.26	0.0026	91.0	1.77
8	0.040	0.10	3.889	14.61	0.17	0.0081	323.8	9.80
9	0.040	0.12	3.542	14.77	0.21	0.0053	212.7	10.82
10	0.040	0.15	1.250	14.61	0.26	0.0027	106.7	4.72
11	0.040	0.20	0.023	14.72	0.34	0.0002	7.7	0.11
12	0.043	0.12	5.018	14.70	0.21	0.0085	366.4	15.26
13	0.045	0.15	2.083	14.56	0.26	0.0013	59.4	7.84

Q_w – water flow discharge; H – the depth of water in the channel in control profile; Q_s – sediment transport discharge; D_* – Bonnefille’s dimensionless grain parameter; $\left(\frac{W}{H}\right)^{-1}$ – inversed width-to-depth ratio; S_0 – energy grade slope line assumption for time $t = t_0$, $y = Q_s \cdot D_* \cdot \left(\frac{W}{H}\right)^{-1}$; and $x = Q_w \cdot S_0$.

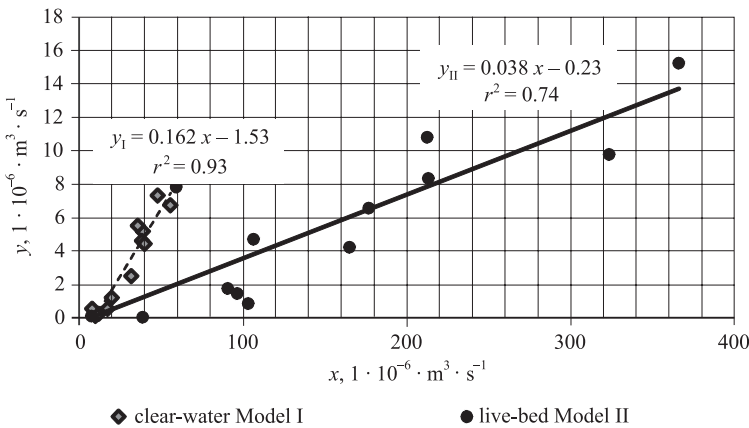


Fig. 9. Modified Lane’s relations graph with the best fit lines, where (x,y) – Modified Lane’s relation coordinates; – line of the best fit between (x,y) for I and II model; r^2 – correlation coefficient

$$y_I = 0.162 x \text{ for model I (clear water conditions)} \quad (14)$$

and

$$y_{II} = 0.038 x \text{ for model II (live-bed conditions)} \quad (15)$$

Verification of modified Lane's relation [Kiraga and Popek 2016] was performed on the basis of real, *in-situ* measured data [Urbański and Hejduk 2014]. Taking into consideration the lack of exact bottom shape data before the flood occurrence, the variability of water surface level during flood conditions, water discharge fluctuations and variable energy grade line slope in natural conditions, the calculation results appears satisfactory, because of the same order of magnitude of values [Kiraga and Popek 2016].

There was attempted to formulate exponential correlation between dimensionless shear stress in bed region θ in D - D cross-section in time $t = t_0$ and mean sediment discharge Q_s and with maximal scour depth z_{\max} for stabilized scour shape in equilibrium conditions (Tab. 5, 6; Fig. 10, 11). To correlate x with y values exponential equations have been derived (Eq. 16–19). Froude number indicate subcritical conditions ($Fr < 1$) for any experimental variant for model I, while in scope of research performed on model II there was almost always subcritical flow, but also supercritical in couple cases ($Fr > 1$).

Table 5. Summary of calculated parameters, connected with hydraulic conditions and sediment properties for Variant I.

Number of measu- rement	Q_w $m^3 \cdot s^{-1}$	H m	u $m^2 \cdot s^{-1}$	Fr –	R_b m	τ_b Pa	θ –	u_* $m^2 \cdot s^{-1}$	Re_* m	θ_{cr} –	z_{\max} m	Q_s $1 \cdot 10^{-6} \cdot m^3 \cdot s^{-1}$
1	0.020	0.10	0.34	0.35	0.0923	0.45	0.045	0.021	12.1	0.032	0.0036	0.059
2	0.025	0.10	0.43	0.44	0.0923	0.72	0.072	0.027	15.3	0.033	0.0200	0.487
3	0.025	0.12	0.36	0.33	0.1088	0.43	0.043	0.021	11.6	0.032	0.0041	0.065
4	0.030	0.10	0.52	0.52	0.0923	1.18	0.117	0.034	19.4	0.034	0.0375	2.056
5	0.030	0.15	0.34	0.28	0.1325	0.52	0.052	0.023	13.0	0.032	0.0030	0.070
6	0.035	0.12	0.50	0.46	0.1088	1.17	0.117	0.034	19.3	0.034	0.0425	1.530
7	0.035	0.15	0.40	0.33	0.1325	0.65	0.065	0.025	14.3	0.033	0.0122	0.150
8	0.040	0.10	0.69	0.70	0.0923	1.09	0.108	0.033	18.5	0.034	0.1061	2.927
9	0.040	0.12	0.57	0.53	0.1088	1.07	0.106	0.033	18.8	0.034	0.0789	1.455
10	0.040	0.15	0.46	0.38	0.1325	1.04	0.104	0.032	18.5	0.034	0.0237	0.660
11	0.040	0.20	0.34	0.25	0.1692	0.33	0.033	0.018	10.4	0.031	0.0039	0.111
12	0.043	0.12	0.62	0.57	0.1088	1.39	0.138	0.037	21.2	0.035	0.0618	2.222
13	0.045	0.15	0.52	0.43	0.1325	1.04	0.104	0.032	18.1	0.034	0.0441	1.471

Table 6. Summary of calculated parameters, connected with hydraulic conditions and sediment properties for Variant II.

Number of measurement	Q_w $m^3 \cdot s^{-1}$	H m	u $m^2 \cdot s^{-1}$	Fr -	R_b m	τ_b Pa	θ -	u_* $m^2 \cdot s^{-1}$	Re_* m	θ_{cr} -	z_{max} m	Q_s $1 \cdot 10^{-6} \cdot m^3 \cdot s^{-1}$
1	0.020	0.10	0.34	0.58	0.0923	4.68	0.466	0.068	38.32	0.037	0.0613	0.347
2	0.025	0.10	0.43	0.72	0.0923	5.98	0.596	0.077	44.16	0.037	0.0872	1.667
3	0.025	0.12	0.36	0.66	0.1088	4.13	0.412	0.064	36.00	0.037	0.0592	0.486
4	0.030	0.10	0.52	0.87	0.0923	5.34	0.532	0.073	41.61	0.037	0.0843	2.597
5	0.030	0.15	0.34	0.71	0.1325	1.69	0.168	0.041	23.47	0.035	0.0270	0.014
6	0.035	0.12	0.50	0.92	0.1088	6.51	0.649	0.081	46.07	0.037	0.0809	2.743
7	0.035	0.15	0.40	0.82	0.1325	3.38	0.337	0.058	33.04	0.036	0.0472	0.465
8	0.040	0.10	0.69	1.15	0.0923	7.33	0.730	0.086	48.30	0.037	0.0870	3.889
9	0.040	0.12	0.57	1.05	0.1088	5.68	0.566	0.075	43.21	0.037	0.0826	3.542
10	0.040	0.15	0.46	0.94	0.1325	3.47	0.345	0.059	33.21	0.036	0.0516	1.250
11	0.040	0.20	0.34	0.82	0.1692	0.32	0.032	0.018	10.19	0.031	0.0142	0.023
12	0.043	0.12	0.62	1.13	0.1088	9.09	0.906	0.095	54.30	0.038	0.0868	5.018
13	0.045	0.15	0.52	1.06	0.1325	1.72	0.171	0.041	23.26	0.035	0.0235	2.083

Q_w – water flow discharge, H – the depth of water in the channel in control profile, u – water flow velocity; Fr – Froude number, R_b – hydraulic radius of the sandy bottom part, τ_b – bed shear stress, θ – dimensionless bed shear stress; u_* – dynamic velocity in velocity field connected with bottom region; R_b – local Reynolds number for bed region; θ_{cr} – critical shear stress (Shield number); Q_s – sediment transport discharge; z_{max} – maximal (equilibrium) scour depth

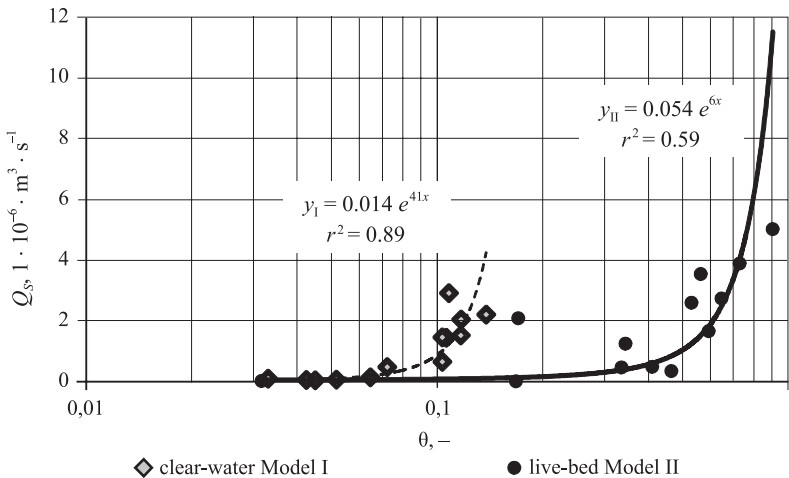


Fig. 10. Dimensionless θ bed shear stress and sediment transport discharge Q_s correlation graph with the best fit lines, $y = a \cdot e^{bx}$ where (x, y) – functions' coordinates, – line of the best fit between (x, y) for I and II model, r^2 – correlation coefficient

$$y_I = 0.014 \cdot e^{41 \cdot x} \text{ for model I (clear water conditions)} \tag{16}$$

and

$$y_{II} = 0.054 \cdot e^{6 \cdot x} \text{ for model II (live-bed conditions)} \tag{17}$$

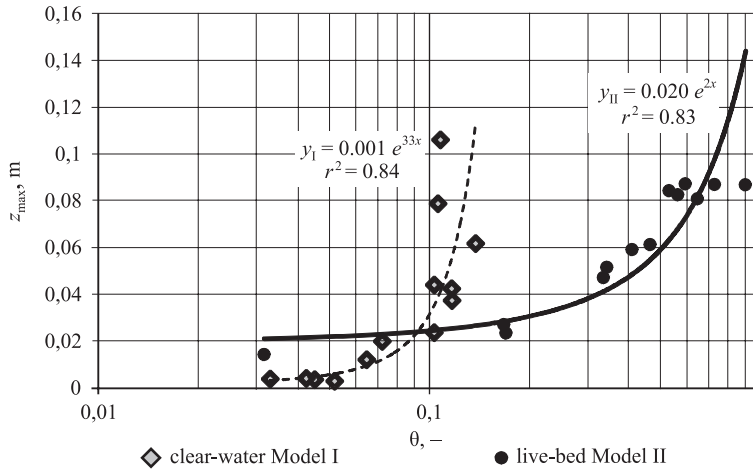


Fig. 11. Maximal scour depth z_{max} and sediment transport discharge Q_s correlation graph with the best fit lines, where (x, y) – functions' coordinates; $y = a \cdot e^{bx}$ – line of the best fit between (x, y) for I and II model; r^2 – correlation coefficient

$$y_I = 0.001 \cdot e^{33 \cdot x} \text{ for model I (clear water conditions)} \tag{18}$$

and

$$y_{II} = 0.020 \cdot e^{2 \cdot x} \text{ for model II (live-bed conditions)} \tag{19}$$

CONCLUSIONS

Lane's relation in its original form has been used as a unique conceptual model in geomorphology and engineering for over 50 years. As well as it was useful in water flow conditions and sediment properties connecting, it is not an equation, but a qualitative expression which cannot be directly used to estimate the influence of a change in one parameter on the magnitude of others, so it has not been recognized as an engineering computation tool so far. Relation is used commonly to describe the natural river morphology forming process and, in consequence, the dynamic equilibrium achieving by natural lowland rivers or mountain streams.

Authors have not found the literature in scope of Lane's relation application in local scour process description or trials to recast it into equation. Also the previous studies of formula modifying are focused on correlate it with geomorphological parameters of the channel [Schumm 1969, Dust and Wohl 2012, Huang et al. 2014]. Concomitantly, the Lane's relation in scope of local scouring in laboratory conditions has not been examined yet.

Modified Lane's relation, presented in paper was examined in steady flow assumption in sub- and supercritical flow conditions. It was two models of bottom structure examined, including clear-water and live-bed local scour forming conditions. The experimental hypothesis was supported – i.e. it could be built a functional relation between right and left side of modified Lane's relation. Also it is possible to use the Lane's relation in local scour forming process description, despite Lane's relation is a principle, commonly used in natural, alluvial rivers morphology forming description, in dynamic balance (equilibrium) conditions. The dynamic balance could be replaced by equilibrium scour depth conditions for local scour forming phenomenon. Also additional relations were discovered – it is also possible to formulate an exponential relation between shear stress and local scour properties (sediment transport discharge and maximal scour hole depth). Almost all functional relationships, both linear and exponential, are based on high-value correlation of dependency (correlation coefficient $r^2 > 0.8$).

The formulated relation was examined in praxis for water flow discharge of $5.06 \text{ m}^3 \cdot \text{s}^{-1}$ in unsteady flow conditions, before and during flood event in case of real object, on the grounds of in-situ measurements [Urbański and Hejduk 2014]. The real objects characteristics were similar to laboratory model I – the solid bottom precedes sandy bed and local scour forming takes place in clear-water conditions. The verification results could be recognized as satisfactory because of the same values' orders of magnitude. Miscalculation could derive from the lack of exact bottom shape data before the flood occurrence, the variability of water surface level during flood conditions, water discharge fluctuations and variable energy grade line slope in natural unsteady flow conditions.

Propitious result of verification in scope of other real objects could be scientific area, that should be further analysed. Other real-object verification tests' results would give data that allow widen the scope of modified Lane's relation components and also additional exponential relations between shear stress and scour properties should be further verified to ensure derived relations.

REFERENCES

- Aderibigbe, O., Rajaratnam, N. (1998). Effect of sediment gradation on erosion by plane turbulent wall jets. *J. Hydr. Engin., ASCE*, 124(10), 1034–1042.
- Barbhuiya, A.K., Dey S. (2004). Local scour at abutments: A review. *Sadhana*, 29(5), 449–476.
- Bollrich, G., Preißler, G. (1992). *Hydromechanik. Band 1*. Verlag für Bauwesen, Berlin.
- Brookes, A. (1988). *Channelized Rivers – Perspectives for Environmental Management*. John Wiley and Sons: Chichester, UK.
- Chabert, J., Engeldinger, P. (1956). *Etude des affouillements autour des piles des ponts*. Laboratoire d'Hydraulique, Chatou.
- Church, M. (1992). Channel morphology and typology. [In:] *The River Handbook*. Vol 1. Eds. P. Calow, G.E. Petts. Blackwell Scientific Publications: Oxford.
- Dąbkowski, Sz.L., Siwicki, P. (2000). Analiza głębokości rozmycia koryta na modelach jazu. *Przegl. Nauk. Wydziału Inżynierii i Kształtowania Środowiska*, 39–50 (in Polish).
- Dust, D., Wohl, E. (2012). Conceptual model for complex river responses using an expanded Lane's relation. *Geomorphology*, 139–140, 109–121

- Gaudio, R., Marion, A. (2003). Time evolution of scouring downstream of bed sills. *J. Hydr. Res.*, 41(3), 271–284.
- Hickin, E.J. (1977). The analysis of river-planform responses to changes in discharge. *River Channel Changes*. Ed. K.J. Gregory. John Wiley and Sons, Chichester.
- Horton, R. (1933). Separate roughness coefficients for channel bottom and sides. *Engin. News Record*, 111(22).
- Huang, H.Q., Liu, X., Nanson, G.C. (2014). Commentary on a “Conceptual model for complex river responses using an expanded Lane’s diagram by David Dust and Ellen Wohl”. *Geomorphology*, 209, 140–142.
- Indlekofer, H. (1981). Überlagerung von Rauigkeitseinflüssen beim Abfluß in offenen Gerinnen. *Mitteilungen Institut für Wasserbau und Wasserwirtschaft. RWTH Aachen*, 37, 105–145.
- Kiraga, M., Popek, Z. (2016). Using a Modified Lane’s Relation in Local Bed Scouring Studies in the Laboratory Channel. *Water*, 8, 16, 1490–1509
- Kubrak, J., Nachlik, E. (2003). *Hydrauliczne podstawy obliczania przepustowości koryt rzecznych*. SGGW, Warszawa (in Polish)
- Lane, E.W. (1955). The importance of fluvial morphology in hydraulic engineering. [In:] *Proc. American Society of Civil Engineers*, New York, 1–17.
- Lenzi, M.A., Marion A., Comiti F., Gaudio R. (2002). Local scouring in low and high gradient streams at bed sills. *J. Hydr. Res.*, 40(6), 731–739.
- Melville, B. (2008). The physics of local scour at bridge piers. *Proc. 4th International Conference on Scour and Erosion*, Tokyo, Japan, 5–7 November 2008.
- Popek, Z. (2006). *Warunki ruchu rumowiska wlezonego w małej rzece nizinnej*. Treatises and Monographs. WULS-SGGW, Warsaw (in Polish)
- Siwicki, P. (2008). Numeryczne modelowanie rozmyć poniżej budowli piętrzących. *Przeł. Nauk., Inżynieria i Kształtowanie Środowiska*, XVII, 2(40), 155–168 (in Polish).
- Siwicki, P., Urbański, J. (2004). Local scour below water structures and their influence on environment. *Acta Sci. Pol., Architectura*, 3(2), 113–120.
- Schumm, S.A. (1969). River metamorphosis. *J. Hydr. Divis. American Society of Civil Engineers*, 95, 255–273
- Schumm, S.A. (1977). *The Fluvial System*. Wiley-Interscience, New York.
- Van Rijn, L.C. (1993). *Principles of sediment transport in rivers, estuaries and coastal seas*. Aqua Publications, Amsterdam.
- Urbański, J., Hejduk, L. (2014). The analysis of local scour size formed after flood event. *Monografie Komitetu Gospodarki Wodnej PAN*, XX (in Polish)
- Warburton, J., Danks, M., Wishart, D. (2002). Stability of an upland gravel-bed stream Swinhope Burn, England. *Catena*, 49, 309–329.
- Zanke, U. (1982). *Grundlagen der Sedimentbewegung*. Springer, Berlin.

WYKORZYSTANIE ZMODYFIKOWANEJ ZALEŻNOŚCI LANE’A DO BADAŃ TWORZENIA SIĘ WYBOJU W KORYCIE ALUWIALNYM

Streszczenie. Lokalne rozmycia dna koryt aluwialnych na odcinku poniżej budowli piętrzących były przedmiotem wielu badań, w których zjawisko tworzenia się wyboju opisywano w różny sposób. W pracy przedstawiono wyniki badań laboratoryjnych, których celem było sprawdzenie możliwości wykorzystania zmodyfikowanej zależności Lane’a do opisu parametrów wyboju w korycie z dnem piaszczystym. Oryginalna zależność Lane’a (1955) opisuje jedynie w sposób jakościowy warunki równowagi dynamicznej aluwialnych koryt rzecznych. W wyniku modyfikacji tej zależności uzyskano równanie, które pozwala na opis ilościowy procesu formowania się rozmycia dna i uzyskania stabilności parame-

trów wyboju w warunkach przepływu ustalonego. Wykonano dwie serie badań na modelu fizycznym koryta o przekroju prostokątnym ze ściankami szklanymi i dnem częściowo lub całkowicie piaszczystym. W I serii badano rozmycia dna w warunkach braku ciągłości transportu rumowiska wlezonego, tj. w korycie, którego dno na początku odcinka pomiarowego było stałe, a na końcu piaszczyste. W II serii badano rozmycia dna poniżej budowli piętrzącej – progu kamiennego z 4 otworami o przekroju prostokątnym. W tej serii badań w rejonie budowli piętrzącej dno było stałe, natomiast powyżej i poniżej spiętrzenia piaszczyste, co zapewniało warunki ciągłości transportu rumowiska wlezonego. Uzyskane wyniki badań potwierdziły możliwość zastosowania zmodyfikowanej zależności Lane'a do opisu charakterystyk rozmycia dna poniżej budowli piętrzących w warunkach równowagi dynamicznej koryta aluwialnego.

Słowa kluczowe: lokalne rozmycie, równowaga dynamiczna, zależność Lane'a, model fizyczny, rzeki aluwialne

Accepted for print – Zaakceptowano do druku: 01.12.2016.

For citation: Kiraga, M., Popek, Z. (2016). Using a modified lane's relation in local bed scouring studies in aluvial bed. *Acta Sci. Pol., Formatio Circumiectus*, 15(4), 209–226.